UNITED STATES DEPARTMENT OF THE INTERIOR

GEOLOGICAL SURVEY

Probabilistic Estimates of Maximum Seismic Horizontal Ground Motion on Rock in Coastal California and the Adjacent Outer Continental Shelf

By

Paul C. Thenhaus, David M. Perkins, Joseph I. Ziony, and S. T. Algermissen

Open File Report 80-924

1980

CONTENTS

Probabilistic Estimates of Maximum Seismic Horizontal Ground Motion on Rock in Western California and the Adjacent Outer Continental Shelf

By

aul C. Thenhaus, David M. Perkins, Joseph I. Ziony, and S. T. Algermissen

ABSTRACT

The regional earthquake shaking hazard has been calculated for coastal California and the adjacent Outer Continental Shelf (OCS) in a series of peak-horizontal-acceleration and peak-horizontal-velocity maps for return periods of approximately 100, 500, and 2500 years. The evaluations are based on a seismogenic zone map that

shows (1) an interlacing system of narrow linear zones that define those major faults associated with earthquakes of moderate to large size, (2) intervening, less-narrow zones of typically lower, more diffuse seismic activity, and (3) other zones of distinctive seismotectonic setting.

For a return period of 100 years, ground motion values calculated at the 90 percent probability level of not being exceeded range as high as 0.59 g and 39 cm/sec, but for most of the offshore area they are less than 0.2 g and 15 cm/sec. Calculated values for a return period of 500 years range as high as 0.78 g and 82 cm/sec, with most of the values offshore less than 0.50 g and 30 cm/sec. For a return period of 2500 years, values as high as 0.82 g and 120 cm/sec are estimated in places, although most of the values offshore are less than 0.60 g and 70 cm/sec.

Two observations are considered in assigning b-values for earthquakes $Ms \geq 4.0$ in areas of low seismic activity. For the more active seismogenic zones, statistical analysis of the historic earthquake record shows a systematic increase in the b-value with increasing distance from the zone of highest strain release in the region. Secondly, samples from simulations of a negative exponential distribution of

magnitude yield b-value estimates lower, on the average, than the underlying b-value of the distribution itself.

Assuming a Poisson model of earthquake occurrence for $Ms \geq 4.0$, we find that 2.3 events of the size $Ms \geq 4.0$ could be expected during the seismic history of a region with a 10 percent probability that no events will actually occur during that time. Using this fact, along with estimates of the times for which the historic record is complete at each magnitude level, the annual rates of earthquakes are estimated for zones where there are no reported historic events ($Ms \geq 4.0$).

Geologically determined recurrence rates for large earthquakes on some of the major faults in western California show relatively good agreement with recurrence rates determined from the historical record of earthquake occurrence, considering the reasonable variability in the numerous assumptions applied in both approaches. Lacking a predictive capacity, a Poisson stochastic process is a reasonable model for earthquake occurrence.

INTRODUCTION

Earthquake shaking hazards in the California OCS are shown in a series of six maps (pls. 2 through 7).

at a scale of 1:5,000,000. The maps show peak-horizontal-acceleration and peak-horizontal-velocity on rock having a 90 percent probability of not being exceeded in 10 years, 50 years, and 250 years; the respective return periods being approximately 100 years, 500 years, and 2,500 years.

The ground motion values presented in this report are intended to be used for purposes related to the mitigation of earthquake risk to buildings normally covered by regular building codes. Because values are determined for bedrock, site specific application would require consideration of thickness and character of overburden and topography. The values on the accompanying maps are obtained from primarily regional considerations and it is therefore to be expected that somewhat different results might be obtained by being more specific about local sources, their maximum magnitudes and seismicity rates. The ground motion maps should be considered lower-bound estimates for the siting of non-critical facilities on bedrock because variability was not incorporated into the attenuation functions; a procedure which results in larger ground motion values.

Estimates of seismicity parameters in this study

are made with due consideration of their importance in the probabilistic method (see Perkins, 1978, McGuire and Shedlock, 1980, McGuire, 1977, McGuire and Barnhard, 1980). In no instance are the seismicity parameters or seismogenic zones intended to be applicable for a deterministic study of design earthquake ground motion. The methodology of the deterministic approach (see Adair, 1979) has been developed for a different set of goals that affect each step of the analysis. Consequently, any part of either analysis is performed under a differing set of assumptions and purposes resulting in different critical input parameters and seismic source zones. Most importantly, the parameters of the deterministic method have a direct impact on the results and therefore have to meet some legally defined standard (see Caggiano, 1979, table 1) whereas the results from this study are far less sensitive to input parameters and therefore need only meet standards of reasonability, convenience and appropriateness to this probabilistic method dealing with short exposure times. It is to this end, of keeping clear distinction between the two methods, that we reserve the label of "seismogenic zones" for the seismic source areas of the probabilistic method. They are

expressly not to be assumed the equivalent of "tectonic province" nor "seismotectonic province" that are terms used in the literature referring to the siting of critical facilities. Also, the maximum magnitudes in this study are not equatable to "maximum credible events". For reasons involving the sensitivity of the results in the probabilistic method explained below, maximum magnitudes in this study may be overestimates of "maximum credible events". Finally, the rates of occurence derived from our fits to historical data may not fairly represent the probability of the next large event in a zone where it is possible to invoke a statistical time-dependent or geophysical predictive model.

The theory and methods used by Algermissen and Perkins (1976) in their probabilistic seismic acceleration map of the contiguous United States are generally followed in this study; however, additions or modifications have been made necessary because of the difference in scale of the hazard mapping. These additions or modifications include more emphasis on geologic factors in seismogenic zoning, a more systematic approach to b-value assessment, and a procedure for determining recurrence rates in zones where earthquakes of $M_s \geq 4.0$ are absent.

McGuire and Shedlock (1980), incorporating uncertainties in input parameters into the probabilistic hazard method, have shown coefficients of variation for 500-year return period values to be between 0.2 and 0.4. As much of this variation comes from attenuation uncertainity, which we have excluded in our studies, the coefficients of variation in the map values of this report are probably significantly less than those cited.

The earthquake catalogue compiled by Algermissen and Rothman and partially listed in Hays and others (1975) has been the source of earthquake data. The catalogue contains historic and instrumental seismicity dating from 1796 through 1974 in the region.

CONSTRUCTION OF SEISMOGENIC ZONES

The probabilistic method used in this study models earthquakes at a set of grid points within the source zones (Algermissen and Perkins, 1976). Because of this, it seems more desirable to model events in areas of similar tectonic and geologic setting rather than in zones that are defined solely on the spatial distribution of seismicity. The assumptions implied by this preferred type of zoning lead to a definition of what we term a seismogenic zone. A seismogenic

zone, as it appears on a map, is a planimetric representation of a three-dimensional domain within the earth's crust within which earthquake potential is assumed to be uniform. That is, earthquakes are assumed to be equally likely throughout the zone and share the same magnitude-frequency relationship.

Faults of regional extent are considered seismogenic zones in themselves where an association between the fault and seismicity can be inferred. This inference may be based on either evidence of historic or Holocene surface faulting on the fault and/or the close spatial association of seismicity with the fault. The boundaries of such seismogenic zones are drawn arbitrarily 10 km either side of the fault in order to enclose the smaller historic earthquakes that may be associated with any particular fault. In this study, no attempt is made to differentiate the segments of individual faults into seperate zones on the basis of different ages of latest displacements. Instead, the occurrence of Holocene or historic rupture along any segment of a fault is taken as an indication that the entire fault is active and that events are equally likely along its entire length.

In areas where individual seismogenic structures of regional extent are not identified, we define zones

assumed to be areas of similar earthquake potential based on similarities in geologic structure and tectonic setting. Several of these zones are relatively large, reflecting our current poor understanding of seismogenic features within them. As additional information becomes available, we would expect that these large zones could be subdivided. The seismogenic zones depicted are based on geologic and seismologic analysis completed in 1978. Geologic data that have become available recently may modify the zone boundaries for parts of the Transverse Ranges and the offshore region.

Southern California and Offshore Borderlands Area

Allen and others (1965) have noted that "most and probably all" of the large historic earthquakes in Southern California that have been associated with surface rupture have occurred on major through going faults having Quaternary movement. Hileman's (1973) presentation of historic seismicity confirms this relationship and also indicates an association of earthquakes as low as magnitude 4 with these faults. Ziony and others (1974) characterize the age of latest movement for faults of coastal

southern California. Their map shows Quaternary and Holocene displacements on the Elsinore (zone 14), Whittier (zone 14, north end), Newport-Inglewood (zones 12 and 13) and the Palos Verdes (zone 13) faults. The fault map of California compiled by Jennings (1975) shows Quaternary movement on both the San Jacinto Fault (zone 15) and the San Andreas Fault (zone 16) south of the Transverse Ranges.

As stated previously, no attempt is made to differentiate the segments of individual faults into separate zones on the basis of different ages of latest displacement. The occurrence of Holocene or historic rupture along any segment of a fault is taken as an indication that the entire fault is active and that events are equally likely along its entire length. There are faults, however, such as the Newport-Inglewood (zones 12 and 13) that have a markedly non-uniform distribution of historic events along them (see Hileman and others, 1973). For these, separate zones are defined based on seismicity so that the recurrence times of this persistent historic activity are not lengthened (thus decreasing the impact on short return-period ground motion maps) by averaging it in with less active areas which cannot be distinguished on a geological basis. We believe that

this procedure more accurately represents the short-term hazard for the areas involved.

Zones in the offshore, continental borderland of Southern California are delineated chiefly on the basis of late Cenozoic fault systems and intervening, relatively unfaulted basinal areas. Vedder and others (1974) suggest an association between seismicity and the offshore faults, particularly the San Clemente-Agua Blanca fault system (zones 1 and 3). Their studies of acoustic profiles indicate a high concentration of faults on the ridges of the Borderland (zones 6 and 7). Junger (1976) has suggested that the ridges of the Borderlands are a product of convergent right lateral faulting at depth and that these faults are not necessarily present at or near the surface. In contrast, the Santa Cruz Basin (zone 9) and San Nicolas Basin (zone 8) show relatively unfaulted basin floors (Vedder and others, 1974) and a relatively lower incidence of seismicity.

Zone 20 contains the San Pedro Basin and the San Diego trough. Although Junger and Wagner (1977) have defined an en echelon fault zone across the San Pedro basin, the area is characterized by only sparse, scattered seismicity. Within the northern part of the San Diego trough, faults are of small vertical

displacement, similar to those in San Pedro basin, and Junger and Wagner (1977) have suggested that the fault trends between the two areas may represent a continuous fault at depth. We have not treated zone 20 as a fault zone because of the diffuse nature of the seismicity and lack of evidence for Holocene or historic movement on the en echelon fault segments. A significantly higher areal rate of activity occurs in the northern San Pedro Basin area which has been seperated into zone 21. Zone 5 ecompasses an undifferentiated area of low seismic activity that includes the Santa Monica Basin, Santa Catalina Island and Catalina Basin. Basins farther seaward on the shelf, the Santa Cruz Basin (zone 9) and the San Nicolas Basin (zone 8) similarly exhibit very little seismicity.

Zone 2 contains the east margin of the San Diego trough and the Coronado Bank. Moore's structure map of the Continental Borderlands (1969, pl.13) shows secondary faults within the zone and Vedder and others (1974) show the Coronado Bank as an uplifted, fault bounded block. The zone has been the site of earthquakes magnitude 5 and greater.

Zone 4 includes the Santa Rosa-Cortes ridge, Tanner and Cortes banks and the East Cortes basin.

Reflection profiling studies by Moore (1969) and Vedder and others (1974) suggest the region is underlain primarily by complicated, large-scale anticlinal folds. Moore (1969) recognized the area as a distinct structural province.

Farther west on shelf, a large zone (zone 10) has been drawn. The paucity of recorded seismicity, along with a lesser degree of detail in the geologic and geophysical studies available, preclude subdivision of zone 10 into smaller zones at this time.

The Western Transverse Ranges

The Western Transverse Ranges contain numerous faults that have been active throughout Quaternary time. The east-west structural grain of the province contrasts with the northwest-oriented structures of the southern California Penninsular Ranges and the Continental Borderland. Whereas the movement on faults south of the Transverse Ranges is primarily right-lateral slip, the Transverse Ranges are characterized by reverse and left-reverse-oblique slip (Jahns, 1973, Wentworth and Yerkes, 1971).

Zone 26 includes the San Fernando fault, which was the site of the 1971 San Fernando earthquake

(M=6.6), and the San Gabriel fault. The latter fault has displaced Pleistocene deposits (Oakeshott (1958), and, although Holocene displacements have not been documented, earthquakes of the size M≥4 have occurred in close proximity to the fault. The remainder of the Transverse Ranges has been subdivided into three regions; a southern zone encompassing the Malibu Coast - Santa Monica fault and the Channel Islands, a central zone containing the Ventura Basin, and a northern zone containing the Santa Ynez Mountains (which includes the Santa Ynez and Big Pine faults).

In discussing the 1973 magnitude 5.2 (Ms) earthquake that occurred seaward of Point Mugu, Ellsworth and others (1973) have called attention to the earthquake hazard of the southern boundary of the Transverse Ranges (zone 23). This boundary is accomodating north-south crustal shortening on north-dipping reverse faults and probably also accomodates some left-lateral slip. The faults comprising this boundary are the Cucamonga, Sierra Madre, Raymond Hill, Santa Monica and Malibu Coast faults. Lee and Vedder (1973) propose a hypothetical continuation of the Santa Monica - Malibu Coast fault system westward as far as the Santa Rosa - Cortes Ridge based on submarine topography and, on the

eastern end of the fault system, Ziony and others (1974) show evidence of Holocene displacement. A marked contrast in seismicity separates the extreme western end of the fault system (zone 41). Although there is little seismic activity in the zone at present, the 1812 earthquake (intensity X) of the Santa Barbara Channel region may have occurred in this zone.

Within the Ventura basin, Hamilton and others (1969) note that seismicity between 1934 -1967 is concentrated in the eastern portion of the Santa Barbara Channel (zone 28) with the western portion (zone 29) being relatively aseismic. Lee and Vedder (1973), reviewing data gathered from 1970 -1971 noticed the same distribution of seismicity. Because of this persistent, non-uniform distribution we have seperated the Ventura basin into three zones (zones 27, 28, and 29) to more accurately represent the historic distribution of seismic activity.

Zone 33 contains the Santa Ynez mountains. The two major structural features of this zone are the Big Pine and Santa Ynez faults. Movements on the faults have been complex but both faults appear to have a component of left-lateral strike-slip. Jennings (1975) indicates Holocene surface rupture along the

Big Pine fault and Lee and Vedder (1973) have noted epicenter locations occuring near the surface traces of both faults.

Central Coastal California and the Adjacent OCS

The chief basis for delineation of seismic source zones in this region are maps by Buchanan-Banks and others (1978).

The Santa Lucia Banks and associated Santa Lucia Banks fault zone defines zone 31. Vrana (1971) inferred that a northeast trend in the seismicity between the latitudes of 34 and 35 north was caused by a splay of the Murray Fracture Zone impinging on the continental slope. However, the northeast trend in the seismicity has been shown to be spurious and caused by the geometry of the network of seismograph stations on land (Gawthrop, 1975). We have zoned in accordance with the work of Gawthrop (1975) who relocated the events using both teleseismic and local data and showed that the events cluster in an area near the Santa Lucia Banks. Gawthrop (1975) summarized a 1969 earthquake sequence (M=5.8 and M=5.4) as right oblique slip on a near-vertical fault of the Santa Lucia Bank fault system, having a rupture

lenght of 20 -25 km.

Along the coast of central California, we have defined the Hosgri fault zone (zone 32) as a seismogenic zone. Relocation of the Lompoc earthquake of November 4, 1927 (M=7.3) by Gawthrop (1975) places the event near the southern terminus of the Hosgri fault zone. Although no historic surface faulting is documented in the offshore area of central California, a fault within the Hosgri fault zone has a minimum age of movement documented as Holocene based on geomorphic evidence although stratigraphic criteria for dating the age of the most recent movement are lacking. Historic seismicity relocated by Gawthrop (1975) shows an association with the Hosgri fault zone. Although there is considerable controversy about the possible connection of the Hosgri and San Gregorio faults, Silver (1978) concludes that the faults are linked and that together they constitute the longest subsidiary fault zone of the San Andreas system. On the basis of this model, we have extended zone 32 northward to include the San Gregorio fault, which has geomorphic evidence and stratigraphic offset that indicate Holocene movement (Buchanan-Banks, 1978).

Zone 34 is an area of complicated geologic structure containing the Santa Lucia Range, Sierra

Madre Range and the San Rafael Mountains. The zone straddles the southwest margin of the Salinian Block; a sliver of continental crust translated to the northwest along the San Andreas fault (Suppe, 1970, Weibe, 1970, Hill, 1971, Johnson and Normark, 1974). The Sur-Nacimiento Fault zone bounds the Salinian Block on the southwest (Page, 1970) and has been the locus of microseismic activity (Gawthrop, 1975). The Rinconada fault within zone 34 also has a high level of microseismicity according to Gawthrop (1975) but neither of these faults have documented Holocene nor historic rupture on them. To the southeast, zone 35, although geologically similar to zone 34, is an area of very low seismic activity. Zone 36 is also part of the Salinian Block however it is distinctive in character because of its low density of faulting and a relatively high rate of seismic activity.

The structure of the shelf off central California has been discussed by Silver and others (1978), Blake and others, (1978), and Hoskins and Griffiths (1971). Zone 37 includes the remainder of the shelf off of central California north to the Mendocino fracture zone. It contains the Santa Maria, Outer Santa Cruz, Bodega, Gualala, and Point Arena basins and the intervening higher areas of the Santa Cruz High and

the Farallon and Oconostata ridges. Major faults bound the Bodega basin but the basin margins show no evidence of deformation in the upper beds of a Plio-Pleistocene sequence (Silver, 1978). A series of faults trend northwest from Point Arena but die out in broad folds on the shelf (Silver, 1978, Hoskins and Griffiths, 1971). The low rate of seismicity in zone 37 precludes seismic parameter distinction among the geologic features in this zone.

Wesson and others (1975) have summarized the evidence for historic, Holocene and Quaternary fault displacements in the San Francisco Bay region. Within historic times earthquakes have been associated with surface rupture on the San Andreas, Hayward, and Calaveras faults and all of these faults have evidence of movement in Holocene time. Zone 38 encloses the Hayward and Calaveras faults and associated seismicity; the bulge of the zone to the east of the Bay area encloses a diffuse pattern of seismicity around the San Pablo Bay area extending eastward to the margin of the Sacramento Valley.

North of the Bay area (zone 39) there is a noticeable drop in the areal rate of seismicity and a much more dispersed pattern to the distribution of seismicity (see Bolt and others, 1968). However, many

faults in the southern part of the area have evidence of Holocene displacement and a coincident alinement of small earthquakes (Wesson and others, 1975). Chapman (1975) has noted a northwest trend in epicenters of minor to moderate shocks in the Clear Lake area which, together with Wesson's information from the faults in the southern portion of the zone, suggests that the northwest trending structures are probably the primary seismogenic features of the zone. The entire zone is one of unusually high heat flow as evidenced by numerous thermal springs (Jennings, 1975) and hydrothermal systems with indicated subsurface temperatures of 90° to 150° C. (Renner and others, 1975).

Zone 24 is the San Andreas fault north of San Bernadino. Numerous historic earthquakes have occurred along this fault and the entire zone shows evidence of Holocene movement. The procedure of differentiating zones of distinctive rates of seismicity was not followed for the San Andreas fault north of the Transverse Ranges (zone 24). There are substantial differences in activity rates and style of deformation along segments of the fault, and equally marked differences in interpretation. On the one hand, Bakun and others (1980) argue that the central,

creeping section of this fault cannot cause high accelerations or large-magnitude events in the future. If we had isolated a low-magnitude, high-rate contemporary-activity zone in this center section, a hazard map would have resulted that depicted relatively high accelerations for short return periods but relatively low accelerations for long return periods. On the other hand, it can be argued, on the basis of the similarity of creep behavior to incipient fracture in metals and rocks, that this region is a likely one for the next large earthquake to occur. (See for example Stuart, 1979.) Burford and Harsh (1980) have addressed this question in terms of stress accumulation and have concluded that between the two hypotheses, a correct choice based on physical arguments is not possible at this time. Accordingly, we treat the entire San Andreas fault as one zone which implies that the creeping section is capable of generating a large magnitude earthquake. This appears to be prudent in light of the conflicting physical arguments.

MODELING OF EARTHQUAKE EVENTS

Where individual faults are identified as seismogenic zones in themselves, the earthquakes of $M_s > 6.4$ are modeled as line sources of appropriate

length directly on the fault. Where possible, in the remaining zones that have earthquakes of $M_s \geq 6.4$ modeled in them, faults not necessarily known to be active at present but with pronounced topographic expression suggestive of relatively recent movement are used as guides to the placement of the line sources (pl. 1). We believe that this procedure, rather than the arbitrary placement of parallel faults spaced 20 km apart (see Algermissen and Perkins, 1976) more accurately represents the state of knowledge of geologic structure in California. All events of the size $M \leq 6.4$ are modeled as point sources and are distributed uniformly throughout the area of a seismogenic zone.

DETERMINING AND ASSIGNING B-VALUES

McGuire and Barnhard (1980) have shown that if b-values can be accurately determined for individual zones, seismic hazard estimates are more accurate than if a single b-value is used for the region. The relatively small size of many of the California source zones resulted in many of the less active zones having only a few historical earthquakes associated with them precluding a direct determination of the b-value. Because in this study source seismicity has been derived from historical rates, we investigated the

properties of b-values (rate of change of occurrence frequency with respect to magnitude) from data samples taken from simulations of a negative exponential distribution of magnitude (the distribution implied by the Richter law). The study showed that as the samples became fewer than 150 events, there was increasing variability in the determined b-value (fig. 1). In addition, for smaller and smaller sample sizes, the 50-percentile b-value estimate is increasingly biased below the true b-value. 75 percent of the samples with fewer than 70 events yielded consistently low estimates of the b-value. This fact was used to evaluate the likely underlying b-value for zones in California where 25-60 events were observed. The curves show percentiles of b-value estimates as a function of sample size for samples taken from a negative exponential simulation with a b-value of 0.6. Estimation was by weighted least squares for data aggregated in 0.6 magnitude intervals. Maximum likelihood estimates using Page's formula (1968) produced equivalent results. The bias in the median estimate is due largely to the aggregation of the data into relatively large ΔM intervals and the placement of the mean magnitude in an interval at the center of the interval.

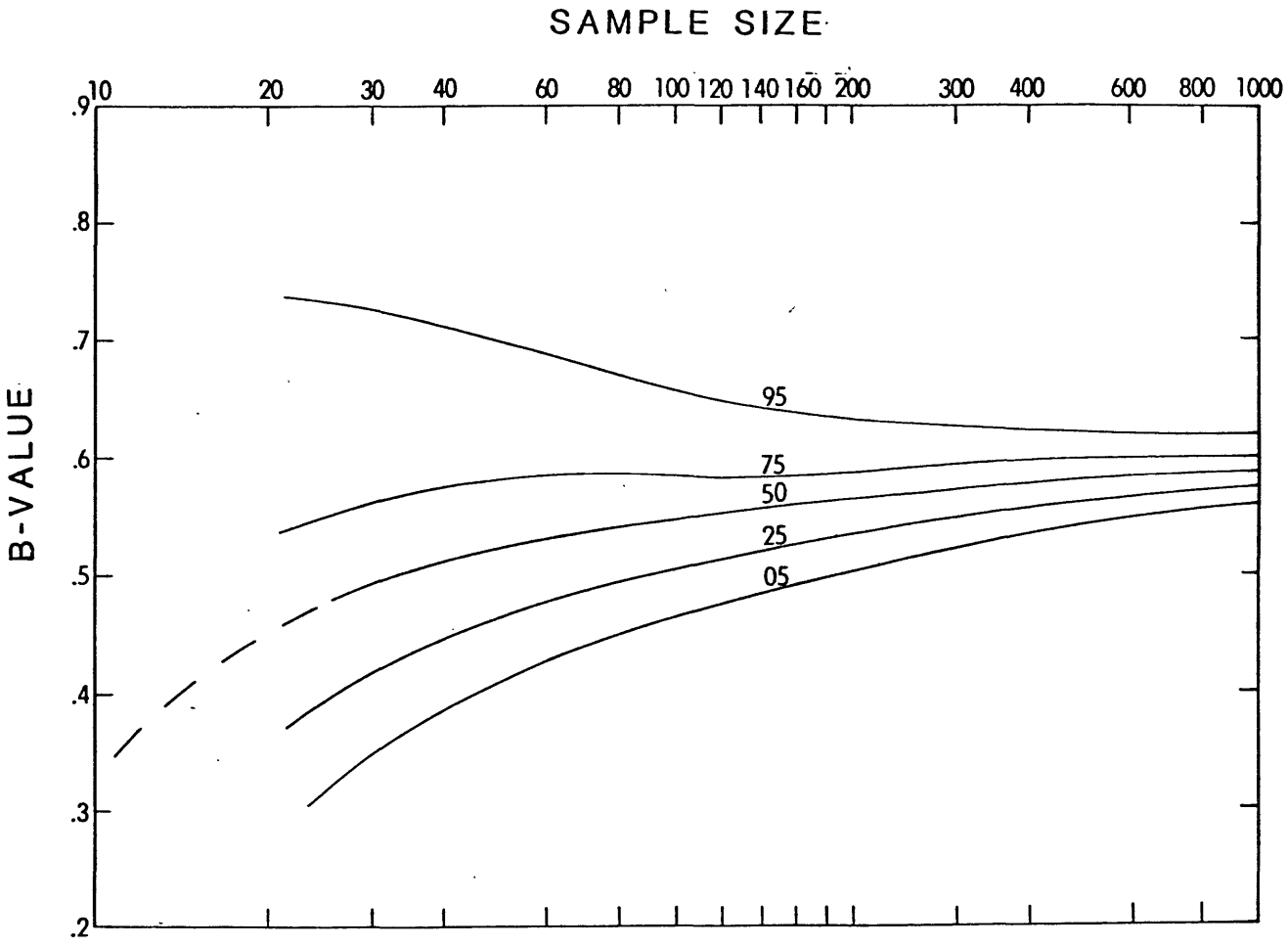

Figure 1.--Estimated b-value as a function of sample size, expressed by percentile curves. At any given sample size, the percentile intercepts give the approximate percent of estimates that do not exceed the intercept value of the b-value axis.

In southern California, b-values of the Elsinore (zone 14) and other parallel seismogenic zones increase in value away from the San Jacinto fault (zone 15)(fig. 2). A similar pattern occurs in west-central California north of the Transverse Ranges. There, the San Andreas fault zone has the lowest b-value with respect to neighboring zones. The pattern observed is consistent with the fact that, historically, the San Andreas and San Jacinto faults have experienced most of the large earthquakes in central and southern California, respectively. That these faults are the principal structures through which strain is released by means of large earthquakes suggests that the strain rate in neighboring zones is lower and therefore accumulated strain is released through relatively infrequent large events. This would result in the zones of lower strain rate having relatively higher b-values. This reasoning is used to infer b-values for other zones having insufficient historical activity to make confident determinations of b-values.

Many zones have less than the minimum number of earthquakes (around 70 events) needed to obtain either a somewhat reliable b-value or a b-value from which one can make an upward adjustment. Given such

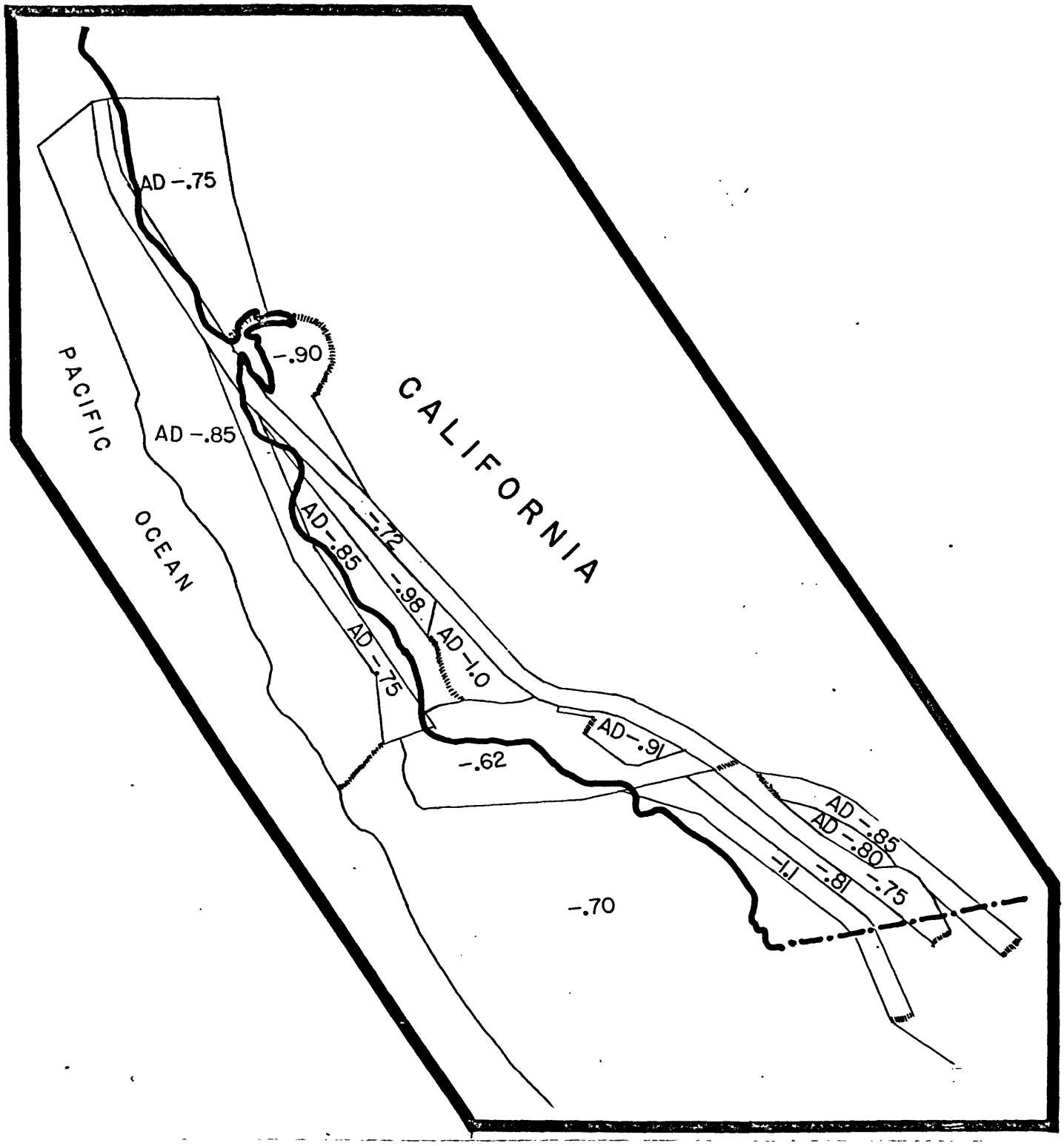

Figure 2.--B-value summary. The b-value applies to all zones within the indicated boundaries. AD indicates that the b-value has been assigned according to the rationale described in the text.

circumstances, the seismicity from zones of similar tectonic setting are combined and the b-value analysis proceeds on the combined set of data. The resulting b-value applies to all the zones used in the combination.

A few zones are geologically unique and are not easily combined with other zones in the study area. An example is the Clear Lake area (zone 39, pl. 1) north of San Francisco Bay. For those areas, b-values are calculated on a less-than-adequate sample to get an idea of a minimum bound for the b-value. B-values are then adopted in accordance with the observation of the central and southern California b-value pattern. These b-values are indicated by the prefix "AD" in figure 2.

Several zones have no earthquakes of $Ms \geq 4.0$. B-values adopted in these zones are consistent with the b-values of neighboring zones and reflect the pattern of strain release in the region.

DETERMINING ANNUAL RATES OF OCCURRENCE

Annual rates of occurrence for the magnitude levels of table 1 are calculated for those zones that have a sufficient number of earthquakes to make possible a judgment on the period of time for which each magnitude level is complete. The annual

Table 1.--Annual occurrence rates for individual seismogenic zones 1-41, shown on plate 1.
[Note: Recurrence interval is the inverse of the annual occurrence rate.]

Zone	b-value	Magnitude intervals							
		$4.0 \leq M_S < 4.6$	$4.6 \leq M_S < 5.2$	$5.2 \leq M_S < 5.8$	$5.8 \leq M_S < 6.4$	$6.4 \leq Ms < 7.0$	$7.0 \leq M_S < 7.6$	$7.6 \leq M_S < 8.2$	$8.2 \leq M_S < 8.8$
		M_c 4.300	4.900	5.500	6.100	6.700	7.300	7.900	8.500
01	-0.70	0.63	0.239	0.091	0.0344	0.0132	0.00502	-------	-------
02	-0.70	0.157	0.060	0.0227	0.0086	0.0031	0.00125	-------	-------
03	-0.70	0.320	0.119	0.0454	0.0172	0.0066	0.00251	-------	-------
04	-0.70	0.320	0.119	0.0454	0.0172	0.0066	0.00251	-------	-------
05	-0.70	0.0484	0.0184	0.0070	0.00265	-------	--------	-------	-------
06	-0.70	0.157	0.060	0.0227	0.0086	0.00331	0.00125	-------	-------
07	-0.70	0.157	0.060	0.0227	0.0086	0.00331	0.00125	-------	-------
08	-0.70	0.0484	0.0184	0.0070	0.00265	--------	--------	-------	-------
09	-0.70	0.0484	0.0184	0.0070	0.00265	--------	--------	-------	-------
10	-0.70	0.182	0.069	0.0263	0.010	--------	--------	-------	-------
11	-0.70	0.77	0.293	0.111	0.0423	0.0161	0.0061	-------	-------
12	-0.70	0.191	0.072	0.0275	0.0105	0.00399	0.00151	-------	-------
13	-0.70	0.358	0.136	0.0518	0.0197	0.0075	0.00284	-------	-------
14	-1.1	0.92	0.201	0.0440	0.0096	0.00211	0.000460	0.000101	-------
15	-0.75	1.49	0.530	0.188	0.067	0.0237	0.0084	0.0029	-------
16	-0.85	0.226	0.0697	0.0215	0.00653	0.00206	0.000635	0.000196	-------
17	-0.80	0.0276	0.0091	0.00303	0.0010	0.000332	0.00019	-------	-------
18	-0.81	1.092	0.357	0.117	0.0381	0.0124	0.0041	-------	-------
19	-0.70	0.320	0.122	0.0462	0.0176	0.0067	-------	-------	-------
20	-0.70	0.193	0.073	0.0279	0.0106	--------	-------	-------	-------
21	-0.70	0.109	0.0414	0.0157	0.0060	-------	-------	-------	-------
22	-0.70	0.0242	0.0092	0.00350	0.00134	-------	-------	-------	-------
23	-0.62	0.117	0.0495	0.0210	0.0089	0.00379	0.00161	0.00069	-------
24	-0.72	1.97	0.74	0.281	0.106	0.040	0.015	0.0057	0.0021
25	-0.91	0.72	0.204	0.058	0.0165	0.00466	0.00141	-------	-------
26	-0.91	0.98	0.277	0.079	0.0224	0.0064	0.00183	-------	-------
27	-0.62	0.0344	0.0146	0.0062	0.00263	0.00112	0.000474	-------	-------
28	-0.62	0.130	0.0552	0.0235	0.0100	0.00424	0.00179	-------	-------
29	-0.62	0.0235	0.0100	0.00424	0.0018	0.00076	0.00033	-------	-------
30	-0.70	0.0363	0.0138	0.00524	0.00199	0.00076	-------	-------	-------
31	-0.85	0.476	0.147	0.0455	0.0141	0.00435	-------	-------	-------
32	-0.75	0.552	0.196	0.070	0.0247	0.0087	0.0031	0.0011	-------
33	-0.62	0.231	0.098	0.0416	0.0177	0.0075	0.00318	0.00136	-------
34	-0.85	0.67	0.207	0.064	0.0198	0.0061	0.0019	0.0006	-------
35	-1.0	0.0233	0.0059	0.00146	0.000365	0.000091	0.0000227	-------	-------
36	-0.98	0.352	0.091	0.0235	0.0061	0.0016	-------	-------	-------
37	-0.85	0.82	0.253	0.078	0.0242	-------	-------	-------	-------
38	-0.90	0.83	0.238	0.069	0.0098	0.0057	0.00165	0.000475	-------
39	-0.75	0.358	0.127	0.0451	0.0016	0.0057	0.00200	0.00072	-------
40	-0.70	0.158	0.060	0.0229	0.0087	-------	-------	-------	-------
41	-0.62	0.084	0.0359	0.0152	0.0065	0.00275	0.00116	0.000489	-------

occurrence rates are estimated by annual averages over the time of completeness for each magnitude level and by the method shown by Stepp (1973). Smoothed occurrence rates are then obtained by fitting the data to the Richter law of occurrence frequencies,

$$\log N = a + bMs$$

where N is the estimated annual rate of earthquakes occurring within the Ms levels specified in table 1. Because many of the earthquakes listed in the catalogue are assigned only epicentral intensity the relationship

$$Ms = 0.6\ Io + 1.3$$

was used to convert epicentral intensities to magnitude. This relationship is also the basis for the magnitude categories in table 1. Applying this relationship to intensities V and higher gives the center magnitudes (Mc) of table 1.

Many of the 41 zones, however, do not have a sufficient number of earthquakes to permit a statement on the length of completeness of the record. For zones where data are insufficient, the seismicity of zones that are similar geologically and that have the same b-value are combined (table 2). From this combined set of events, the length of completeness for each magnitude level of interest can be estimated and

Table 2.--Zone combinations chosen to determine annual occurrence rates

Areas Combined	Numbers of zones combined (see plate 1)		
Southern California Borderland ridges	1	4	
	2	6	
	3	7	
Remaining Southern California Borderland zones	5	10	21
	8	19	22
	9	20	40
Rose Canyon, Newport-Inglewood, and Palos Verdes fault zones	11		
	12		
	13		
Western Transverse Ranges	23	33	
	27	41	
	28		
San Gabriel fault and adjacent zone	25		
	26		
Central outer-continental shelf	31		
	37		

the annual occurrence rates for the combined set of events calculated. These rates are smoothed, as before, and the resulting smoothed annual rates are then back-allocated to the original seismogenic zones so that the amount of seismic activity back- allocated is approximately equal to the proportion of the zone's original contribution of earthquake events to the combined smoothing process.

Zones 25, 30, and 35 (pl. 1) have no earthquakes of the size $Ms \geq 4.0$. To determine occurrence rates for these zones, we pose a simple probabilistic argument: regardless of magnitude, how many earthquakes could be expected in such a zone and still have a random 10 percent chance of none occurring during the seismic history? Ten percent is a common significance level used in testing statistical hypotheses. The usual procedure in testing hypotheses is to assert a hypothesis and, assuming this hypothesis to be true, construct a statistic. If the observed statistic is more infrequent than that possible by chance at the given level of significance, the assumed hypothesis is rejected. . Our procedure reverses the process. We assume that the statistic "zero occurred" lies at the level of significance of the hypothesis and, working backwards, determine the parameter (expected number to

occur) of the assumption, given Poisson occurrences. Thus:

$$P(0 \text{ occurrences, given } \lambda) = 0.10$$
$$\Rightarrow \lambda = 2.3$$

To calculate rates for the magnitude levels of table 1, the length of time for which each of the magnitude levels is completely reported needs to be determined. The earliest dates at which these levels could be completely reported are estimated from the surrounding zones, from historical rates of population settlement, from isoseismal extent for various magnitudes, and from isoseismal patterns observed from neighboring zones. We then have the expression

$$y_1 \cdot r_{4.3} + y_2 \cdot r_{4.9} + y_3 \cdot r_{5.5} + \ldots + \ldots = 2.3 \qquad (1)$$

where y_i is the estimated number of years for which the corresponding magnitude level is completely reported and r is the annual rate of earthquake occurrence at that magnitude level.

The rates of each of the given magnitude levels are related by the equation:

$$\frac{r_{i+1}}{r_i} = 10^{b\Delta m} \qquad (2)$$

where b is the b-value and $\Delta m = 0.6$ for the magnitude intervals of the assumed log-frequency graphs. Substituting into equation 1) and letting α equal the annual rate of the magnitude 4.3 level, the equation becomes:

$$\alpha \left[\sum_{i=1}^{n} y_i (10^{b\Delta m})^{(i-1)} \right] = 2.3$$

$$\alpha = \frac{2.3}{\sum_{i=1}^{n} y_i (10^{b\Delta m})^{(i-1)}}$$

where i indicates the corresponding magnitude level from 1, indicating the 4.3 level, 2 indicating the 4.9 level, to the highest magnitude level assigned to the seismogenic zone.

Once α is determined, $r_1 = \alpha$ and the rates for the various magnitude levels can then be found by successive multiplication using equation 2).

MAXIMUM MAGNITUDE

Our primary aim in assigning maximum magnitudes is to assess the largest possible earthquake magnitude for a seismogenic zone to the extent that the value would significantly affect probabilistic ground motions. Sensitivity studies (Perkins, 1978) suggest that once values of magnitude 7 are reached

progressively higher maximum magnitudes produce correspondingly lower factors of increase in the ground motions at a given return period. Thus, if maximum magnitudes are sufficiently high, the issue of the exact value is no longer very critical for a probabilistic study. In the context of this study, it is sufficient that maximum magnitudes be reasonable in the light of 1) historical seismicity and 2) geologic framework.

To satisfy the constraint of historical seismicity, we require that the adopted maximum magnitude in a source zone be at least as high as the historical maximum magnitude experienced in that zone. However the largest observed earthquake may be much less than the potential maximum if the period of observation is less than the recurrence time of the maximum event. This is particularly a problem for small source zones which result from detailed geologic zoning. However, by identifying families of similar fault types or extensions of fault systems, we can estimate the historical maximum for the families as a whole and adopt that same maximum for members having only low levels of seismicity.

To satisfy the requirement of geologic framework, regressions of magnitude on fault rupture length

served as a guide. They could only be used as a general guide, however, because of two problems with the use of such regressions. First, there is the uncertainty of what percentage length of fault might rupture in any event. In this study we considered lengths from one-half the fault length to the entire length of the fault. Second, given a maximum possible rupture length, the regressions only give an average magnitude. Probabilistic maximum magnitudes at the 90 or 95 percentile from these regressions would be perhaps a magnitude unit higher, corresponding to values so high as to be unreasonable. In summary then, maximum magnitudes are magnitudes that are equal to, or somewhat higher than, that experienced historically and are also equal to, or somewhat larger than, that suggested by a regression for a rupture between one-half to the whole length of the zone's longest fault. For further discussion of our treatment of maximum magnitudes, we will refer to the maximum magnitudes assigned in the above manner as "tentative maximum magnitudes".

Once a tentative maximum magnitude is adopted for a zone, we have to incorporate this estimate into the discrete magnitude categories of table 1, which as previously stated, were derived from the intensity-Ms

relationship. The center magnitude, Mc, designates the Ms category comprising earthquakes having magnitudes between Mc - 0.3 and Mc + 0.3. Thus the "effective" maximum magnitude in any Mc category is Mc + 0.3. A problem arises in relating the tentative maximum magnitude to an appropriate maximum Mc category. Three cases can be identified: 1) The tentative maximum magnitude is equal to or just a little less than some Mc + 0.3. In this case it is clearly appropriate to adopt this Mc as the maximum Mc. 2) The tentative maximum magnitude is nearly equal to some Mc. If we adopt this Mc as the maximum Mc, the "effective" maximum magnitude is two to three tenths magnitude unit higher than the tentative maximum magnitude. This is acceptable, because measured magnitudes have an average error around one-quarter magnitude unit, and our tentative maximum magnitude is a relatively uncertain estimate anyway. 3) The tentative maximum magnitude is a little larger than some Mc - 0.3. This case provides two choices: either adopt this Mc, making the effective maximum magnitude four to five tenths magnitude unit higher than the tentative maximum magnitude, or, adopt the next lower Mc, impeaching the tentative maximum magnitude with the arguments concerning the

variability of instrumental magnitudes or uncertainties in obtaining the tentative maximum magnitude from fault information. We chose not to have an effective maximum magnitude lower than the tentative one, and so adopted the former, somewhat conservative course of action. Thus, in the following discussion, maximum Mc indicates the Ms category in which the tentative maximum magnitude fell, and the "effective" maximum magnitude is given by the maximum Mc + 0.3. The procedure is ad hoc, in some cases producing larger-than-maximum-credible magnitudes for some "effective" upper-bound magnitudes. Neither these nor the maximum Mc's should be considered appropriate for assessment of design earthquakes for structures.

Using the above rationale, a maximum Mc=7.9 was assigned to the San Jacinto fault of southern California (fig. 3). The largest observed historic event in the zone was the Imperial Valley earthquake of 1940, magnitude 7.0 and was accompanied by approximately 25 km of surface rupture having right lateral displacement (Buwalda and Richter, 1941). Mark and Bonilla's regression of magnitude on fault length for strike-slip faults (1977) yields a most likely size of about M=7.7 for an event of one-half

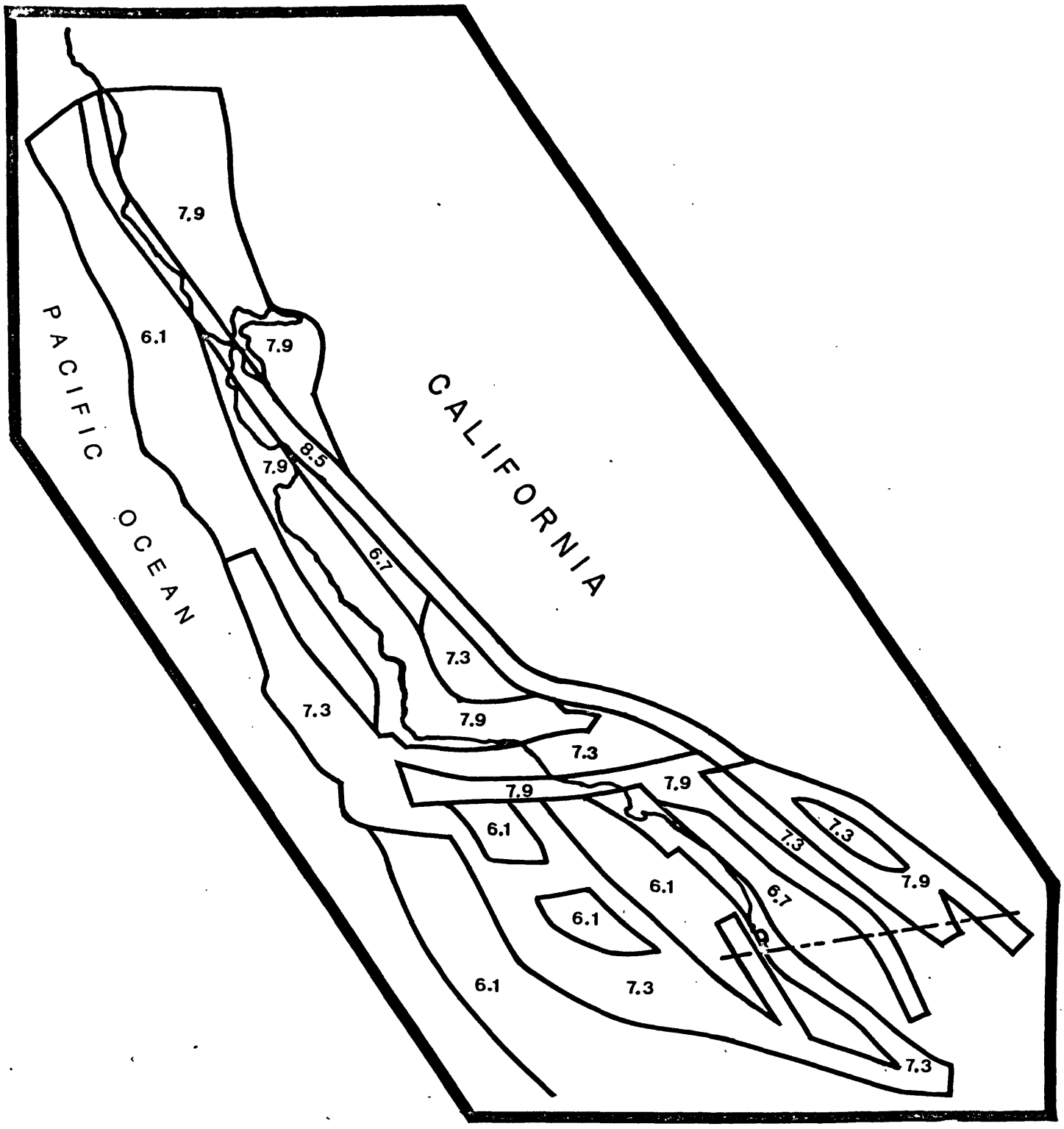

Figure 3. -- Summary of estimated maximum M_c for seismogenic zones in the study area. The values shown apply to all of the zones within the indicated boundaries.

the fault length. A maximum Mc of 7.9 therefore is not unreasonable to assume. Because the southern San Andreas and Elsinore faults are also characterized by right-lateral stike-slip movement and similarly, are large, through-going faults, they too were assigned the maximum Mc=7.9.

The 1940 Imperial Valley earthquake occurred on a prviously unsuspected fault (Buwalda and Richter, 1941), which may be considered a branch of the San Jacinto (Allen and others, 1965). Because strain release between the Pacific and North American plates is taking place over a broad region in southern California, we have estimated relatively high values of maximum Mc in the inter-fault seismogenic zones 17 and 18.

West of the Elsinore, a second group of fault zones has been assigned a maximum Mc of Mc=7.3. This center magnitude includes a magnitude 7.6 event that occurred on the Agua Blanca fault. The second largest event among these zones was the 1933 magnitude 6.3 earthquake that occurred on the Newport-Inglewood fault (Barrows, 1974). Because we feel that the primary seismogenic structures have been included in the foregoing group of faults, the maximum Mc values adopted for the remainder of the shelf in southern

California is accordingly lower. The largest recorded events in zones 20 and 21 are magnitude 4.6 earthquakes. The assigned maximum Mc is well in excess of the observed historic magnitudes, yet it is reasonable in light of the possibility of there being undiscovered faults, or greater continuity of fault systems, in areas where geologic and geophysical investigations are sketchy at present.

The northern and southern zones of the western Transverse Ranges (zones 33 and 41) have been assigned a maximum Mc of 7.9. The intensity X 1812 (estimated M=7.3) event may have been located in the southern frontal zone of the Transverse Ranges (zone 41). Three intensity VIII events (M=6.1) have occurred in zone 33. We have assigned a maximum Mc considerably higher than the largest historic event because of the lengths of the Santa Ynez fault (~150 km) and the Big Pine fault (~75 km). Mark and Bonilla's regression of magnitude on fault length for strike-slip fault data indicates that the most likely size for an event with a rupture length of 75 km (approximately one- half the length of the Santa Ynez fault) is a magnitude 7.3. A somewhat higher estimate, M=7.5 is credible if normal oblique-slip has characterized the fault's movement. Because this is a mean estimate of the size of events

rupturing that fault length, a value of the size maximum Mc=7.9 is not unreasonable.

The Ventura Basin area experienced a magnitude 6.3 event in 1925 and a magnitude 6.0 event in 1941. Earthquake epicenters have been associated with segments of the Red Mountain, Pitas Point-Ventura and San Cayetano faults (Lee and others, 1978) and the region has geologic evidence of late Quaternary fault movement (Ziony and others, 1974, Howell, 1978). Lee and Ellsworth (1975) suggested 7.5 as a maximum credible earthquake in the Santa Barbara Channel region which is consistent with our assigned maximum Mc of 7.3.

Offshore of central California, a maximum Mc=7.3 has been adopted for along the Santa Lucia High. This is consistent with the values assigned to the faulted ridges elsewhere on the shelf. The remainder of the shelf, exclusive of the Hosgri-San Gregorio fault zone, has been assigned maximum Mc=6.1. This is consistent with the less faulted, less active areas of the Continental Borderlands area of Southern California. For the present study, a maximum Mc of 7.9 has been assigned to the San Gregorio and Hosgri faults based on the assumption that they are linked segments of a continuous fault zone. However, if an

alternate model of seperate en-echelon faults is accepted, maximum Mc values of 7.3 could be appropriate for each fault. This same value (Mc=7.9) was applied to the area east of the Hosgri that contains the Sur-Nacimiento and Rinconada faults. Microseismic activity suggests that these faults are probably seismogenic features, although no Holocene or historic movement has been documented on them. If they are seismogenic, each fault is long enough to be considered capable of possibly generating a high-magnitude earthquake.

The eastern portion of the Salinian Block (zone 36) is anomalous, as mentioned previously, because of its relatively unfaulted nature as compared to the surrounding terranes. Although the zone has a relatively high rate of activity for lower magnitude events ($M<5$), it is not considered capable of generating a large event due to a lack of large scale faulting. Zone 35, on the other hand, is an area that is seismically quiet but has faults of intermediate length with Quaternary movement (Jennings, 1975). One of these, the Ozena fault could be a splay of the Rinconada fault system. We have assigned the zone a maximum Mc of 7.3.

The largest historic event east of the San

Andreas fault in central California the intensity IX (estimated M=6.7) 1868 event on the Hayward fault. If one assumes that the Hayward and Healdsburg-Rodgers Creek are a continuous feature of length 163 km (Wesson and others, 1975, table 1), a rupture of one half that length yields a most likely magnitude of 7.3 using the regression of Mark and Bonilla (1977) for strike slip data. It is not unreasonable therefore, that a maximum Mc=7.9 be adopted. Because it is probable that the fault systems are continuous between zones 38 and 39, the same value has been applied to zone 39.

The San Andreas fault (zone 24) has been assigned the highest maximum Mc of western California, with a maximum Mc of 8.5. The great 1906 San Francisco earthquake (M=8.3) occurred in this zone and is thought to be near the probable maximum magnitude event for the zone.

CALCULATION OF ESTIMATED GROUND MOTION

The a-value, and b-value (from the Richter law previously mentioned) and maximum magnitude are parameters which characterize our estimate of the annual rates of occurrence for future earthquakes in any particular zone. These parameters are used to calculate the estimated annual occurrences for the

various magnitude ranges in table 1. The procedure (Algermissen and Perkins, 1976) distributes earthquakes uniformly throughout a zone, and, at every point on a map grid, calculates the accelerations produced by these earthquakes using the acceleration attenuation functions of Schnabel and Seed (1973). For the velocity maps, an interim velocity attenuation by D.M. Perkins, S.T. Harding and S.C. Harmsen (written commun., 1979) was used. These ground motions have the same annual occurrence rates as the magnitudes that produce them. The successive application of this procedure for every possible earthquake location in the zone, for every magnitude at these locations, and for every zone in the region, produces a histogram of acceleration occurrences at every map grid point. The histogram can be turned into a cumulative probability distribution, which, in turn, is used to calculate exceedance probabilities for various exposure times. Each map is the result of contouring the values of the acceleration at each grid point for a given probability of exceedance during a given exposure time. In this report we present maps (pls. 3 - 8) showing accelerations having only a 10 percent probability of being exceeded in 10, 50, and 250 years. For convenience the maps have been titled

with the approximate return periods (the inverse of annual probability of exceedance) and are so referred to later in this text. The relationship between exceedance probability, r, of an acceleration value, a, in exposure time, T, and the return period, R, of acceleration a is given by the equation,

$$1-r_T(a) = e^{-\frac{T}{R(a)}}$$
$$= e^{-(\text{annual rate of exceedance of a}) \cdot T}$$

The exact (rather than approximate) return periods of the accelerations on the maps are 95, 475, and 2,372 years. The approximate values come from the handy rule of thumb

$$r_T(a) \simeq \frac{T}{R(a)}$$

which holds when $T \lesssim 0.1\ R$.

GENERAL CHARACTER OF THE MAPS

The level of detail chosen to perform the ground motion mapping, appropriately represents the present state of knowledge of the seismotectonics of California. Had larger zones been used we would have masked distinctions in both geology and seismicity that we think are important to highlight. Whether these distinctions result in contrasts in seismic

hazard depends upon the rates of seismic activity, the return period selected, and the character of the attenuation function used.

Greater detail in zoning than we have provided would require a level of geologic and seismologic that is not generally available for much of the study area. Also, because the epicentral location accuracy is about 5 or 10 km for most of the coastal area, it would be difficult to associate historic earthquake activity with smaller seismogenic zones.

The detail of the maps increases with increasing return period (pls. 3 - 8). The 100-year return-period map (pl. 3) shows acceleration values between 4 and 30 percent g. These levels of acceleration are experienced as far as 100 km from most sources. As a result, the map resembles a smoothing of the source regions. On the other hand, the 2,500-year return-period map (pl. 5) shows accelerations generally 30 to 60 percent g. These higher accelerations are experienced only within 15 km from the higher magnitude earthquakes, so that the contours of the acceleration maps closely approximate the geometric shape of the delineated seismogenic zone.

Algermissen and Perkins (1976) and Perkins (1978)

have shown that an increase in the return period by a factor of five approximately doubles the peak acceleration for low to moderate accelerations. This rule of thumb can be observed by comparing the 100-year and 500-year return-period acceleration maps.

By comparing the 500- and 2,500-year return-period maps it can be seen that an increase of a factor of five in return period does not constitute as much as a doubling of the acceleration. The factor of increase becomes instead roughly 1.5 for the lower accelerations and about 1.2 for the higher accelerations in the 500-year map. The accelerations at the the longer return periods are dominated by the higher ground motions that are governed by the higher magnitude events. The accelerations produced by the higher magnitude events asymptotically approach the value of the acceleration produced by the maximum credible event. Therefore, the factor of increase in acceleration between the 500-year and 2,500-year map will be smaller for those zones that are already experiencing near-maximum magnitude events at the 500-year return-period level. Also, because we are mapping accelerations that have a constant probability of exceedance (10 percent in a given exposure time), increasing the frequency of near-maximum magnitude

events in zones that already have recurrences for these events of less than 2,500 years will not effect a significant change in the 2,500-year return-period map. Hence, the discrepancies between the recurrence rates shown in tables 3 and 4 will produce little change in the 2,500-year return-period map.

Because of the longer predominant periods of peak velocities as compared to acceleration attenuations, the velocity attenuations have a slower decrease with distance for a given magnitude and a greater ratio in the near field between a given pair of magnitudes. Accordingly, in comparing the acceleration and velocity maps at a given return period we should expect more smoothness in the velocity map but greater contrast in values between zones of different maximum magnitudes. Neither of these are evident in the 100-year return period maps, but in the 2500-year return period maps the contrast is quite evident. The smoothing and contrasting effect apparently counteract one another over most of the map, and at return periods for which maximum local ground motions are likely to be evident, the contrasting effect predominates. Thus, in general, the accelerations and velocity maps are quite similar in form, especially if contour values have been selected to reflect geologic

framework.

COMPARISON OF EARTHQUAKE RECURRENCE RATES DETERMINED FROM GEOLOGIC INFORMATION WITH RECURRENCE RATES DETERMINED FROM HISTORIC SEISMICITY

As ground motion mapping becomes more detailed, fewer historic events are contained in the progressively smaller seismogenic zones. It then is desirable to consider the rates of seismic activity that would be suggested by geologic evidence. The geologically determined seismic history would not only aid the calculation of rates for zones having sparse historical activity but also would give perspective on the question of whether historical seismicity is representative of the seismicity of the geologic past.

Several methods of determining earthquake recurrence intervals from geologic data have been used recently (Anderson, 1979; Molnar, 1979; Sieh, 1978; Sims, 1975). Varied assumptions are applied in using these methods and yield results that differ from one another significantly.

Molnar (1979) derived a relative frequency relationship for earthquakes using the average rate of slip on a fault and empiric expressions relating fault

displacement, magnitude, and seismic moment. Using the slip rates given by Anderson (1979) for faults in western California and substituting our b-values and effective maximum magnitudes in the moment equations of Molnar (1979), annual occurrence rates are calculated. Table 3 is a comparison between the rates predicted by average annual fault slip and from historic seismicity. The comparison shows the largest discrepancy between the two methods on the southern San Andreas fault. The geologically determined slip rate indicates that the southern San Andreas should be much more active than historic seismicity indicates. Anderson (1979) noted this same discrepancy. On the northern San Andreas, the recurrence rates calculated from historic seismicity show a somewhat more frequent occurrence of events as compared to occurrence rates derived from geologically-determined slip rates.

An alternative comparison is possible based on estimated recurrences inferred from offsets of strata exposed in trenches across faults. Along the San Andreas fault at Pallett Creek, Sieh (1978) has found geologic evidence for perhaps as many as eight earthquakes comparable in size to the 1857 event ($M_s \geq 8.25$). The "uniform earthquake model" Sieh proposed from this evidence is that events of a size

Table 3.--Comparison between rates predicted by geologically-determined annual fault slip and by historic seismicity.

Faults	b-value (from table 1)	Annual slip moment[1] (dyne-cm/yr)	Maximum magnitude, (M_m)	Maximum magnitude in terms of moment	Magnitude of interest (M_I)	Moment of interest	Annual rates $M_m \geq M \geq M_I$ moment	historic	Ratio moment : historic
San Andreas west of Sierra Nevada	-0.72	7.9×10^{25}	8.8	1.8×10^{29}	≥ 7.9 ≥ 4.9	$\geq 7.9 \times 10^{27}$ $\geq 2.5 \times 10^{23}$	0.0012 0.1479	[2]0.0014 [2]0.2341	1: 1.2 1: 1.6
San Andreas south of Transverse Ranges	-0.85	1.4×10^{25}	8.2	2.24×10^{28}	≥ 7.9 ≥ 4.9	$\geq 7.9 \times 10^{27}$ $\geq 2.5 \times 10^{23}$	0.00049 0.1739	0.00011 0.0561	4.5: 1 3.1: 1
San Jacinto	-0.75	2.2×10^{25}	8.2	2.24×10^{28}	≥ 7.9 ≥ 4.9	$\geq 7.9 \times 10^{27}$ $\geq 2.5 \times 10^{23}$	0.00087 0.1470	0.0015 0.4875	1: 1.8 1: 3.3
Elsinore	-1.1	1.1×10^{24}	8.2	2.24×10^{28}	≥ 7.9 ≥ 4.9	$\geq 7.9 \times 10^{27}$ $\geq 2.5 \times 10^{23}$	0.000028 0.0559	0.000048 0.1205	1: 1.7 1: 2.2
San Gregorio Hosgri	-0.75	1.7×10^{25}	8.2	2.24×10^{28}	≥ 7.9 ≥ 4.9	$\geq 7.9 \times 10^{27}$ $\geq 2.5 \times 10^{23}$	0.00064 0.1136	0.00023 0.0640	2.8: 1 1.8: 1

[1] From Anderson (1979).
[2] Normalized to a length of fault from San Luis Obispo to Cajon Pass, which was used for fault moment calculation by Anderson (1979).

comparable to the 1857 event dominate 300 km of the south-central portion of the San Andreas and have an average recurrence of 160 years. Two of the geologically inferred events do not have clearly definitive evidence of being as large as magnitude 8. Consequently, it is possible that the recurrence for magnitude 8 events is somewhat longer than 160 years. To have a basis for comparison to the rates of the San Andreas both north and east of the Transverse Ranges (zone 24), Sieh's rates were considered to be a sampling of a 300 km length of the fault; comparable to the length of rupture of the 1857 event. Because zone 24 is about 900 km long, increasing Sieh's annual occurrence rates by a factor of three would normalize them to the 900 km fault length (table 4). This, of course, implies that Sieh's rates are uniform along the San Andreas fault. This assumption could be contradicted, based upon proposed physical models of the San Andreas fault (Citron and Turcotte, 1976; Hill, 1974), but, owing a lack of geologic recurrence data from elsewhere on the fault, this assumption presently cannot be improved upon. Applying the rate in the above manner appears to produce a conservative estimate (short recurrence intervals) for recurrences of large events along the fault (tables 3 and 4).

Table 4.--Comparison of earthquake recurrences on the San Andreas fault as determined from geologic data of Sieh, 1978, and from historic seismicity.

(Note: Recurrence interval is the inverse of the annual rates.)

	Annual Rates		
	M>8	M>7.9	Ratio
Hypothesis	Geologic	Historic	Geologic:Historic
1. All geologic earthquakes are M>8.0 and comparable to the 1857 event (Sieh's uniform earthquake model)	0.0188	0.0042	4.5: 1
2. Seven of the nine events (inclusive of the 1857 earthquake) are M>8.0	0.015	0.0042	3.6: 1
3. Five of the nine events (inclusive of the 1857 earthquake) are M>8.0 (Seih's uniform slip model)	0.0101	0.0042	2.4: 1

Sieh's second hypothesis is the "uniform slip model". In this model four of the events are hypothesized to be M≳7.0 and occur in time between the truly great earthquakes. This model brings the annual occurrence rates from the geologic data and from our treatment of historical data into the best agreement (table 4). If the M≳7.0 events of the uniform slip model are considered a complete sampling of M≳7.0 events though, the geologically derived average recurrence interval for events of this size is 10 times longer than the recurrence intervals predicted from the historic record.

It should be noted though, that if all eight of the geologic events are assumed to be as low as M≳7.0, the annual rates of occurence, as determined by the two methods are in close agreement.

We can get a feel for the sensitivity of the relationship between magnitude and annual occurrence rates by recalling equation 2).

$$\frac{r_{i+1}}{r_i} = 10^{b\Delta m}$$

By trying to assign a magnitude (x) to the geologic events, so that the predicted geologic rate now

associated with M>8 (r_8) is the same as for the historic rates of M>7.9, equation 2) becomes:

$$\frac{r_8}{r_x} = 10^{b(8-x)} \qquad 3)$$

From 3) it can be shown that with a b-value of -0.72 for a magnitude decrease of 0.5, the factor of decrease for the occurrence rate is 2.3. Hence, in Sieh's uniform slip model a decrease in the magnitude of the events by 0.5 would bring the geologic rates into good agreement with the historic rates. Good agreement could also be achieved between the uniform earthquake model and historic rates if the magnitude of the proposed great events is decreased by one. A decrease of one in magnitude results in a factor of five decrease in annual occurrence rates for a b-value of -0.72. This effect of magnitude on occurrence rate is even more pronounced at higher b-values. Hence, any comparison between recurrences from geologic seismicity and historic seismicity is highly dependent on the interpreted magnitude of the event inferred from geologic relations observed within a trench. Because of the numerous qualitative judgments involved in likening the size of a number of the geologic

events to the 1857 event, we feel that a variability of one-half to one magnitude unit for these events is not at all unreasonable to assume. Therefore, we do not consider Seih's rates as substantially different from the historic seismicity rates as we have treated them. It is noteworthy that our estimates of seismicity rates for the northern San Andreas, based on historic seismicity, lies between the rates indicated by presently available geologic methods (tables 3 and 4).

It cannot be assumed a-priori that the accuracy of the hazard estimate is increased by using geologically determined recurrence of large earthquakes in a short-exposure-time study as this. Insights gained from studies using the Chinese earthquake catalogue (that has historically observed earthquakes dating from 1350 ad.) indicate that the most recent past is the best indicator of seismic activity in the near future (McGuire, 1979, McGuire and Barnhard, 1980). This is because indiscriminant use of a long earthquake history could average through several cycles of seismic activity, each lasting several centuries, resulting in a less accurate estimate of the activity in the near future. Rates for 50 year intervals taken from the high and low

portions of a cycle may differ by a factor of 10 while the difference in rates through successive 50 year intervals may be a factor of 2 or less. The critical questions in a short-exposure-time study are 1) what is the rate of activity in the current cycle and 2) on what part of the present cycle are we? Answers to these questions would invoke a predictive, time-dependent model. At present, a time-dependent statistical model might be viable only on the northern San Andreas near Fort Tejon due to the data collected by Sieh (1978). At best the model would apply to only large events. On the southern San Andreas, the descrepancy between the historic rates of seismicity and the rates indicated from geologically-determined slip rates might be an indication of seismic periodicity on that fault. If this is the case, it is not clear whether the current activity is marking the end or the begining of a relatively more active stage. Assuming the former, the near future activity could be expected to remain the same or decrease. Assuming the latter, an increase over the historic rate might be expected in the near future or perhaps even that a large earthquake is imminent. Because of considerable controversy involved with such modelling we chose not to use time-dependent models in this study.

In the absence of a predictive capacity, a Poisson model of occurrence is reasonable (McGuire and Barnhard, 1980). This point is further supported by the fact that the current rate of relative plate motion has been the same over 4.5 million years (Atwater and Molnar, 1973) and available data indicate generally good agreement between seismicity indicated by moments derived from this plate interaction and historic seismicity when judged against differences in rates of seismicity through the cycles of the Chinese earthquake catalogue.

MAPPED ACCELERATIONS AS LOWER-BOUND HAZARD ESTIMATES

Given the source zones and their seismicity parameters, we must point out that the acceleration and velocity values derived from them in this study are not conservative (i.e., unreasonably high). The calculations were made without taking into account statistical variability in 1) the attenuation function, 2) the maximum magnitudes, and 3) the fault length versus magnitude relationship. Incorporating estimates of these variabilities would spread the acceleration histograms and therefore produce an

increase in the calculated acceleration at a given level of extreme probability.

We believe that the maps (pls. 2 - 7) depict suitable values for a lower-bound estimate of seismic ground-shaking hazard on rock at a site. More detailed studies could establish lower values of acceleration and velocity if:

1) earthquakes larger than M = 6.4 occur farther from the site than on the faults chosen in the model;

2) earthquakes smaller than M = 6.4 do not occur relatively uniformly in a zone but preferentially at some distance removed from the site;

3) earthquake rates for the same or similar source zones are less than those adopted. For accelerations from 4 percent to 30 percent g, rates 70 percent of those used will produce accelerations of only about 85 percent of the mapped values;

4) maximum magnitudes are 6.0 or lower. Our maximum magnitudes are 6.4 or higher, and, generally, above 6.4, only maximum magnitudes that are greatly different from those adopted would produce a substantial change from the mapped values.

REFERENCES CITED

Adair, Merlyn J., 1979, Geologic evaluation of a site for a nuclear power plant, in, Hatheway, A. W., and McClure, C. R., Jr., eds.: Geology in the siting of nuclear power plants, Geological Society of America, Reviews in Engineering Geology, v. 4, p. 27-39.

Algermissen, S. T., and Perkins, D. M., 1976, A probabilistic estimate of maximum accleration in rock in the contiguous United States: U.S. Geological Survey Open-File Report 76-416, 45 p.

Allen, R. C., St. Amond, P., Richter, C. F., and Nordquist, J. M., 1965, Relationship between seismicity and geologic structure in the southern California region: Seismological Society of America Bulletin, v. 55, no. 4, p. 753-797.

Anderson, J. G., 1979, Estimating the seismicity from geological structure for seismic-risk studies: Seismological Society of America Bulletin, v. 69, no. 1, p. 135-158.

Atwater, T., and Molnar, P., 1973, Relative motion of the Pacific and North American plates deduced from sea floor spreading in the Atlantic, Indian and South Pacific oceans, in, Proceedings of the Conference on Tectonic Problems of the San Andreas Fault system, R. L. Kovach and A. Nur, eds., v. XIII, Stanford University Publications, v. 13, p. 136-148.

Bakun, W. H., Stewart, R. M., Bufe, C. B., and Marks, S. M., 1980, Implication of seismicity for failure of a portion of the San Andreas fault: Seismological Society of America Bulletin, in press.

Barrows, A. G., 1974, A review of the geology and earthquake history of the Newport-Inglewood structural zone, southern California: California Division of Mines and Geology, Special Report 114.

Blake, M. C., Jr., Campbell, R. H., Dibblee, T. W., Jr., Howell, D. G., Nilsen, T. H., Normark, W. R., Vedder, J. C., and Silver, E. A., 1978, Neogene basin formation in relation to plate-tectonic evolution of San Andreas fault system, California: American Association of Petroleum Geologists Bulletin, v. 62, no. 3, p. 344-372.

Bolt, B. A., Lomnitz, C., and McEvilly, T. V., 1968, Seismological evidence on the tectonics of central and northern California and the Mendocino escarpment: Seismological Society of America Bulletin, v. 58, no. 6, p. 1725-1754.

Buchanan-Banks, J. M., Pampeyan, E. H., Wagner, H. C., McCulloch, D. S., 1978, Preliminary map showing recency of faulting in coastal south-central California: U.S. Geological Survey Miscellaneous Field Studies Map, MF-910, 3 pl., scale 1:500,000.

Burford, R. O., and Harsh, P. W., 1980, Slip on the San Andreas fault in central California from alinement array surveys: Seismological Society of America Bulletin, in press.

Buwalda, J. P., and Richter, C. F., 1941, Abstract, Imperial Valley earthquake of May 18, 1940: Geological Society of America Bulletin, v. 52, p. 1944-1945.

Caggiano, J. A., Jr., 1979, A three-phase program of investigation for site selection and development, in, Hatheway, A. W., and McClure, C. R., Jr., eds.: Geology in the siting of nuclear power plants, Geological Society of America, Reviews in Engineering Geology, v. 4, p. 13-25.

Chapman, R. H., 1975, Geophysical study of the Clear Lake region, California: Division of Mines and Geology Special Report 116, 23 p.

Citron, G. P., and Turcotte, D. L., 1977, Curvature of the San Andreas fault, California--Comment and Reply: Geology, v. 5, no. 6, p. 324-325.

Ellsworth, W. L., Campbell, R. H., Hill, D. P., Page, R. A., Alewine, R. W., III, Hanks, T.C. Heaton, T. H., Hileman, J. A., Kanamori, H., Minster, B., and Whitcomb, J. H., 1973, Point Mugu, California, earthquake of 21 February 1973 and its aftershocks: Science, v. 182, no. 4117, p. 127-1129.

Gawthrop, W., 1975, Seismicity of the central California coastal region: U.S. Geological Survey Open-File Report 75-134, 48 p.

Hamilton, R. M., Yerkes, R. F., Brown, R. D., Jr., Burford, R. O.,DeNoyer, J. M., 1969, Seismicity and associated effects, Santa Barbara region, in Geology, Petroleum development and seismicity of the Santa Barbara channel region, California: U.S. Geological Survey Professional Paper 679, p. 47-77.

Hays, W. W., Algermissen, S. T., Espinosa, A. F., Perkins, D. M., Rinehart, W. A., 1975, Guidelines for developing design earthquake response spectra: Construction Engineering Research Laboratory Technical Report M-114, p. 155-314.

Hileman, J. A., Allen, C. R., and Nordquist, J. M., 1973, Seismicity of the southern California region 1 January 1932 to 31 December 1972: Seismological Laboratory, California Institute of Technology, Pasadena, Calif.

Hill, M. L., 1971, A test of new global tectonics: Comparisons of northeast Pacific and California structures: American Association of Petroleum Geologists Bulletin, v. 55, no. 1, p. 3-9.

Hill, M. L., 1974, Is the San Andreas a transform fault?: Geology, v. 2, no. 11, p. 535-536.

Hoskins, E. G., and Griffiths, J. R., 1971, Hydrocarbon potential of northern and central California offshore, in Cram, I. H., ed.: Future petroleum provinces of the United States--their geology and potential, American Association of Petroleum Geologists, Memoir 15, v. 1, p. 212-228.

Howell, D. G., McCulloch, D. S., and Vedder, J. G., 1978, General geology, petroleum appraisal and nature of environmental hazards, eastern Pacific shelf, latitude 28° to 38° north: U.S. Geological Survey Circular 786.

Jahns, R. H., 1973, Tectonic evolution of the transverse ranges province as related to the San Andreas fault system, in Proceedings of the Conference on Tectonic Problems of the San Andreas Fault System: Stanford University Geological Science Publication, v. 13, p. 149-170.

Jennings, C. W., 1975, Fault map of California with locations of volcanoes, thermal springs and thermal wells: California Division of Mines and Geology, scale 1:750,000, one sheet.

Johnson, J. D., and Normark, 1974, Neogene tectonic evolution of the Salinian block, west-central California: Geology, v. 2, p. 1-14.

Junger, A., 1976, Tectonics of the southern California borderland, in Howell, D. G., ed., Aspects of the geologic history of the California continental borderland: American Association of Petroleum Geologists, Pacific Section, Miscellaneous Publication 24, p. 486-598.

Junger, A., and Wagner, H. C., 1977, Geology of the Santa Monica and San Pedro Basins, California continental borderland: U.S. Geological Survey Miscellaneous Field Studies Report 820, 10 p.

Lee, W. K., and Vedder, J. G., 1973, Recent earthquake activity in the Santa Barbara channel region: Seismological Society of America Bulletin, v. 63, no. 5, p. 1757-1773.

Lee, W. K., and Ellsworth, W. L., 1975, Earthquake activity in the Santa Barbara channel region, in Oil and gas development in the Santa Barbara channel outer continental shelf off California: U.S. Geological Survey Environmental Statement, p. 11-80 to 11-137.

Lee, W. K., Johnson, C. E., Henyey, T. L., Yerkes, R. L., 1978, A preliminary study of the Santa Barbara, California, earthquake of August 13, 1978 and its major aftershocks: U.S. Geological Survey Circular 797, 11 p.

Mark, R. K., and Bonilla, M. G., 1977, Regression analysis of earthquake magnitude and surface fault length using the 1970 data of Bonilla and Buchanan: U.S. Geological Survey Open-File Report 77-614, 8 p.

McGuire, R. K., 1977, Insights from the Chinese earthquake catalogue on seismic hazard assessment: U.S. Geological Survey Open-FileReport 77-715, 30 p.

McGuire, R. K., and Barnhard, T. P., 1980, Effects of temporal variations in seismicity on seismic hazard: Seismological Society of America Bulletin, in press.

McGuire, R. K., and Shedlock, K. M., 1980, Statistical uncertainties in seismic hazard evaluations in the United States: Seismological Society of America Bulletin, in press.

Molnar, P., 1979, Earthquake recurrence intervals and plate tectonics: Seismological Society of America Bulletin, v. 69, no. 1, p. 115-133.

Moore, D. G., 1969, Reflection profiling studies of the California continental borderland: Structure and Quaternary turbidite basin: Geological Society of America Special Paper 197, 142 p.

Oakeshott, G. B., 1958, Geology and mineral deposits of San Fernando quadrangle, Los Angeles County, California: California Division of Mines and Geology Bulletin 172, 147 p.

Page, B. M., 1970, Sur-Nacimiento fault zone of California: Continental margin tectonics: Geologic Society of America Bulletin, v. 81, p. 667-690.

Page, R., 1968, Aftershocks and microaftershocks of the great Alaska earthquake of 1964: Seismological Society of America Bulletin, v. 58, no. 3, p. 1131-1168.

Perkins, D. M., 1978, Acceleration hazard map sensititivity to input seismic parameters: Bolletino Di Geofisica Teorica Ed Applicata, v. 20, no. 78, p. 188-196.

Rehner, J. L., White, D. E., Williams, D. L., 1975, Hydrothermal convection systems in White, D. E., and Williams, D. L., eds., Assessment of geothermal resources of the United States: U.S. Geological Survey Circular 726, p. 5-59.

Schnabel, P. B., and Seed, H. B., 1973, Accelerations in rock for earthquakes in the Western United States: Seismological Society of America Bulletin, v. 63, p. 501-516.

Sieh, K. E., 1978, Prehistoric large earthquakes produced by slip on the San Andreas fault at Pallett Creek, California: Journal of Geophysical Research, v. 83, no. 88, p. 3907-3939.

Silver, E. A., 1978, Geophysical studies and tectonic development of the continental margin off the Western United States, lat. 34° to 48° N., in Cenozoic tectonics and regional geophysics of the Western Cordillera; Smith, R. B., and Eaton, G. P., eds., Geological society of America Memoir 152, p. 251-262.

Silver, E. A., 1978, The San Gregorio-Hosgri Fault Zone: An overview, in Silver, E. A., and Normark, W. R., eds., The San Gregorio-Hosgri Fault Zone: California Division of Mines and Geology, Special Publication 137, p. 1-2.

Silver, E. A., McCulloch, D. S., Curray, J. R., in preparation, Marine geology and tectonic history of the central California continental margin, 55 p.

Sims, J. D., 1975, Determining earthquake recurrence intervals from deformational structures in young lacustrine sediments: Tectonophysics, v. 29, p. 141-152.

Stepp, J. C., 1973, Analysis of completeness of the earthquake sample in the Puget Sound area, in Harding, S. T., ed., Contributions to seismic zoning: National Oceanic and Atmospheric Administration Technical Report ERL267-ESL30, p. 16-28.

Stuart, W. D., 1979, Strain softening prior to two-dimensional strike-slip earthquakes: Journal of Geological Research, v. 84, n. B3, p. 1063.

Suppe, J., 1970, Offset of late Mesozoic basement terrains by the San Andreas fault system: Geological Society of America Bulletin, v. 81, p. 3253-3258.

Vedder, J. G., Beyer, L. A., Junger, G. W., Moore, G. W., Roberts, A. E., Taylor, J. C., and Wagner, H. C., 1974, Preliminary report on the geology of the continental borderland of southern California: U.S. Geological Survey, Miscellaneous Field Studies Report 624, 34 p.

Vrana, R. S., 1971, Seismic activity near the eastern end of the Murray Fracture Zone: Geological Society of America Bulletin, v. 82, p. 789-792.

Weibe, R. A., 1970, Pre-Cenozoic tectonic history of the Salinian block, western California: Geological Society of America, v. 81, p. 1837-1842.

Wentworth, C. M., and Yerkes, R. F., 1971, Geologic setting and activity of faults in the San Fernando area, California in The San Fernando, California earthquake of February 9, 1971: U.S. Geological Survey Professional Paper 733, p. 6-16.

Wesson, R. L., Helley, E. J., LaJoie, K. R., and Wentworth, C. M., 1975, Faults and future earthquakes, in Borcherdt, R. D., ed., Studies for seismic zonation of the San Francisco Bay region, 1975: Geological Survey Professional Paper 941-A, p. A5-A30.

Ziony, J. I., Wentworth, C. M., Buchanan-Banks, J. M., and Wagner, H. C., 1974, Preliminary map showing recency of faulting in coastal southern California: U.S. Geological Survey Miscellaneous Field Studies Report MF-585, 3 pl., scale 1:500,000, 7 p.